

# Eigenvalue Decomposition Approach for Beampattern Synthesis

Jie Chen<sup>1</sup> and Yingzeng Yin<sup>2</sup>

<sup>1</sup>School of Electronic Engineering  
Xi'an Aeronautical University, Xi'an, 710077, China  
chenbinglin88888@163.com

<sup>2</sup>National Key Laboratory of Antenna and Microwave Technology  
School of Electronic Engineering, Xidian University, Xi'an, 710071, China  
yyzeng@mail.xidian.edu.cn

**Abstract** — The relation between the manifold matrix of the array and the synthesized beampattern is investigated. The synthesized beampattern can be obtained by eigenvalue decomposition of the projection matrix of the array manifold matrix, while the least square error reaches the minimum. For an antenna array whose manifold matrix has been determined, the projection matrix can be derived easily from the array manifold matrix. Then, eigenvalue decomposition of the projection matrix is implemented to obtain the synthesized beampattern. The antenna element excitations can be obtained by an ameliorated least square method. The results of the simulations compared with the traditional least square method show that the matching degree between the targeted beampattern and the synthesized beampattern of the new method is higher and that the new method is more efficient.

**Index Terms** — Array manifold matrix, beampattern synthesis, eigenvalue decomposition, least square method, projection matrix.

## I. INTRODUCTION

Beampattern synthesis of the antenna array and beamforming technology have been broadly studied and used in the domains of multiple-input multiple-output (MIMO) radar and smart antenna for several decades. In the early phase of development, beamforming was accomplished in the radio frequency front end by phase shifters and radio amplifiers weighting the antenna element excitations. This structure is cumbersome, sizable, and inflexible. As microelectronic and digital technology develop, beamforming is achieved by digital signal processing techniques. The most researched topic is the receiving beamforming, in which the received antenna element signals are weighted to form the expected beampattern. Many approaches for beamforming have been developed by researchers. One method is the well-known capon beamforming [1,16].

Another approach views beamforming as a nonlinear optimization problem to obtain the antenna element excitations or the weighting vector. This method has been used in several recent studies [2-7]. However, it is well known that convex optimization approach is an iterative method for pattern synthesis in most cases.

Currently, with the development of signal processing technology, many articles have been published. In the literature [8], an optimization method of an arbitrary side-lobe attenuation level was provided. The literature [9] discussed a beamforming approach for wideband use in MIMO systems. In the literature [10], a compressed sensing method was applied for beamforming. An ameliorated difference genetic algorithm for beamforming was proposed in the literature [11]. In the literature [12], the beamforming method under the constraint of  $l_1$ -norm minimization was investigated. Phased array beam steering through serial control of the phase shifters was presented in another article [13].

The least square (LS) method is a classic approach that has been used broadly in many areas [14]. A steerable least square approach was presented in a further article [15]. Reference [17] studied the phase and pattern characteristics of a sub-wavelength broadband reflectarray unit element based on triple concentric circular-rings.

In the methods mentioned above, the expected beampatterns are often presumed in advance as a determined vector to lower the complexity of beamforming and to reduce the computing amount. However, none of these methods investigates the relation between the manifold matrix of array and the targeted beampattern. In this paper, the relation between the manifold matrix of array and the targeted beampattern is investigated. The synthesized beampattern can be obtained by eigenvalue decomposition of the projection matrix of the array manifold matrix, while the least square error reaches the minimum. Then, the

antenna element excitations can be obtained through an ameliorated least square method. Compared with the traditional least square method, the synthesized outcomes of the new approach are more efficient and have better agreement with the expected beampattern. In addition, the new method is a non-iterative approach for pattern synthesis.

The rest of this paper is organized as follows: Section II presents the beampattern synthesis paradigm; Section III provides the eigenvalue decomposition method for beampattern synthesis; Section IV shows the solution of the array excitation by an ameliorated least square method; Section V discusses the new approach and compares the results with the traditional least square method; and Section VI draws a conclusion.

## II. BEAMPATTERN SYNTHESIS PARADIGM

Consider an  $N$ -element  $d$ -spaced uniform linear antenna array, where all the elements are isotropic. Assume all the antenna elements transmit a narrow-band beam with a central wave length  $\lambda$ . We investigate the far-field scenario. The antenna elements are arranged as shown in Fig. 1, numbered from 1 to  $N$ .

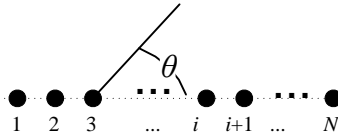


Fig. 1. Arrangement of the uniform linear antenna array.

In Fig. 1, the angle between the signal and the axis of the array is denoted as  $\theta$ , in the far field, the formed beampattern can be written as:

$$s = \sum_{i=0}^{N-1} W_i e^{j2\pi i d \cos \theta / \lambda}. \quad (1)$$

In equation (1),  $W_i$  is the  $i+1$ <sup>th</sup> antenna element's current excitation.

Let  $\mathbf{a}(\theta) = [1, e^{j2\pi d \cos \theta / \lambda}, \dots, e^{j2\pi d(N-1) \cos \theta / \lambda}]^T$  be the steering vector with superscript  $T$  denoting the transpose operation. Denote the antenna element excitation vector as  $\mathbf{W} = [W_0, W_1, \dots, W_{i-1}, \dots, W_{N-1}]^T$ . Thus, equation (1) can be expressed as:

$$s = \mathbf{a}^T(\theta) \mathbf{W}. \quad (2)$$

Set  $\theta$  in the interval of  $[0^\circ, 180^\circ]$ . Denote its discrete value as  $\theta_1, \theta_2, \dots, \theta_k, \dots, \theta_K$ . If the targeted beampattern vector is:

$$\begin{aligned} \mathbf{P} &= [P(\theta_1), P(\theta_2), \dots, P(\theta_k), \dots, P(\theta_K)]^T \\ &= [P_1, P_2, \dots, P_k, \dots, P_K]^T, \end{aligned} \quad (3)$$

then, the objective of the beampattern synthesis is to obtain the weighting vector by solving the equation:

$$\text{abs}([\mathbf{a}(\theta_1), \mathbf{a}(\theta_2), \dots, \mathbf{a}(\theta_k), \dots, \mathbf{a}(\theta_K)]^T \mathbf{W}) = \mathbf{P}, \quad (4)$$

where  $\text{abs}$  denotes the absolute value operation.

Let  $\mathbf{A} = [\mathbf{a}(\theta_1), \mathbf{a}(\theta_2), \dots, \mathbf{a}(\theta_k), \dots, \mathbf{a}(\theta_K)]$ , where  $\mathbf{A}$  is the array manifold matrix; therefore, equation (4) can be expressed as:

$$\text{abs}(\mathbf{A}^T \mathbf{W}) = \mathbf{P}. \quad (5)$$

It is difficult to solve this equation directly because this equation is considered an overdetermined equation in most cases.

To solve this equation, traditional practice is to transform equation (5) into either:

$$\mathbf{A}^T \mathbf{W} = \mathbf{P}, \quad (6)$$

or

$$\min \|\mathbf{A}^T \mathbf{W} - \mathbf{P}\|^2. \quad (7)$$

In equation (7),  $\|\cdot\|$  denotes the vector length operation.

Compared with equation (5), equations (6) and (7) remove the absolute value operation and simplify the solving process. There are many traditional methods to solve equations (6) and (7). Obviously, removing the absolute operation of equation (5) largely simplifies the process, however, it also causes less agreement between the synthesized beampattern and the expected beampattern. Hence, in the following sections of this paper, a novel approach is presented to solve equation (5).

## III. BEAMPATTERN SYNTHESIS BY EIGENVALUE DECOMPOSITION

To solve equation (5), an intermediate vector  $\mathbf{F}$  is used to satisfy:

$$\mathbf{A}^T \mathbf{W} = \mathbf{F}, \quad (8)$$

$$\text{abs}(\mathbf{F}) = \mathbf{P}. \quad (9)$$

First, equation (9) can be solved; its solution is:

$$\begin{aligned} \mathbf{F} &= \text{diag}(e^{j\phi_1}, e^{j\phi_2}, \dots, e^{j\phi_K}) \mathbf{P} \\ &= [P_1 e^{j\phi_1}, P_2 e^{j\phi_2}, \dots, P_K e^{j\phi_K}]^T. \end{aligned} \quad (10)$$

In this equation,  $\text{diag}$  denotes the diagonal matrix, and  $\phi_k$  ( $k=1, 2, \dots, K$ ) is an arbitrary angle variable. Therefore, we can obtain:

$$\text{diag}(\mathbf{F}^*) = \text{diag}[P_1 e^{-j\phi_1}, P_2 e^{-j\phi_2}, \dots, P_K e^{-j\phi_K}]^T, \quad (11)$$

where  $*$  denotes the conjugate operation.

Then, equation (9) can be transformed into:

$$\begin{aligned} \text{diag}(\mathbf{F}^*) \mathbf{F} &= \text{diag}[P_1 e^{-j\phi_1}, P_2 e^{-j\phi_2}, \dots, P_K e^{-j\phi_K}]^T \mathbf{F} \\ &= [P_1^2, P_2^2, \dots, P_K^2]^T = \text{diag}[P_1, P_2, \dots, P_K]^T \mathbf{P} \\ &= \text{diag}(\mathbf{P}) \mathbf{P}. \end{aligned} \quad (12)$$

Hence, equation (8) can be transformed into:

$$\text{diag}(\mathbf{F}^*) \mathbf{A}^T \mathbf{W} = \text{diag}(\mathbf{F}^*) \mathbf{F} = \text{diag}(\mathbf{P}) \mathbf{P}. \quad (13)$$

Denote  $\mathbf{G} = \text{diag}(\mathbf{F}^*) \mathbf{A}^T$  and  $\mathbf{M} = \text{diag}(\mathbf{P}) \mathbf{P}$ . Then, equation (13) can be rewritten as:

$$\mathbf{G} \mathbf{W} = \mathbf{M}. \quad (14)$$

Its least square solution is:

$$\mathbf{W}_{\text{LS}} = (\mathbf{G}^H \mathbf{G})^{-1} \mathbf{G}^H \mathbf{M}. \quad (15)$$

In equation (15), superscript  $H$  denotes the conjugate transpose operation.

According to the projection theory, equation (15) means that while  $\mathbf{M}$  is projected into the column vector space of the  $\mathbf{G}$  matrix, the error between the synthesized beampattern obtained by  $\mathbf{W}_{LS}$  and  $\mathbf{M}$  reaches the minimum [14]. It is easy to determine that the projection vector from  $\mathbf{M}$  to matrix  $\mathbf{G}$ 's column vector space is [14]:

$$\mathbf{P}_G = \mathbf{G}(\mathbf{G}^H \mathbf{G})^{-1} \mathbf{G}^H \mathbf{M}. \quad (16)$$

Its error vector is [14]:

$$\mathbf{E}_G = (\mathbf{E} - \mathbf{G}(\mathbf{G}^H \mathbf{G})^{-1} \mathbf{G}^H) \mathbf{M}, \quad (17)$$

where  $\mathbf{E}$  is a unit matrix.

Obviously, the minimum of the error is  $\mathbf{0}$  vector, i.e.,  $\mathbf{E}_G = \mathbf{0}$ . Hence, in this situation:

$$\mathbf{E}_G = (\mathbf{E} - \mathbf{G}(\mathbf{G}^H \mathbf{G})^{-1} \mathbf{G}^H) \mathbf{M} = \mathbf{0}. \quad (18)$$

Taking a step forward, we can obtain:

$$\mathbf{G}(\mathbf{G}^H \mathbf{G})^{-1} \mathbf{G}^H \mathbf{M} = \mathbf{E} \mathbf{M} = \mathbf{1} \times \mathbf{M}. \quad (19)$$

Equation (19) means  $\mathbf{M}$  is the eigenvector of the matrix  $\mathbf{G}(\mathbf{G}^H \mathbf{G})^{-1} \mathbf{G}^H$  to the eigenvalue of 1.

Therefore, the synthesized beampattern  $\mathbf{Q}$  can be obtained from the eigenvalue decomposition of the matrix  $\mathbf{G}(\mathbf{G}^H \mathbf{G})^{-1} \mathbf{G}^H$ .  $\mathbf{Q}$  is the eigenvector to the eigenvalue of 1. From  $\mathbf{Q}$ , the array element excitation vector can be obtained.

#### IV. THE SOLUTION OF THE ELEMENT CURRENT EXCITATIONS

After eigenvector  $\mathbf{Q}$  is substituted into equation (14), the following equation can be obtained:

$$\mathbf{G} \mathbf{W} = \mathbf{Q}. \quad (20)$$

Substituting  $\mathbf{G} = \text{diag}(\mathbf{F}^*) \mathbf{A}^T$  into equation (20), we can obtain:

$$\mathbf{G} \mathbf{W} = \text{diag}(\mathbf{F}^*) \mathbf{A}^T \mathbf{W} = \mathbf{Q}. \quad (21)$$

From equation (21), we can obtain:

$$\mathbf{A}^T \mathbf{W} = (\text{diag}(\mathbf{F}^*))^{-1} \mathbf{Q}. \quad (22)$$

Let  $\mathbf{D} = \text{diag}((\text{diag}(\mathbf{F}^*))^{-1} \mathbf{Q})$  and  $\mathbf{B} = \mathbf{A}^T$ ; then, the steerable least square solution  $\mathbf{W}$  of equation (22) can be obtained as [15]:

$$\mathbf{W} = (\mathbf{B}^H (\mathbf{D}^{-1})' \mathbf{B})^{-1} \mathbf{B}^H (\text{diag}(\mathbf{F}^*))^{-1} \mathbf{Q}, \quad (23)$$

where  $l$  is an integer variable.

#### V. THE SIMULATIONS AND RESULTS

In this section, three examples are conducted to demonstrate the new approach's performance.

Consider an  $N$ -element  $d$ -spaced uniform linear antenna array, where all the elements are isotropic. Assume all the antenna elements transmit a narrow-band beam with a central wave length  $\lambda$ . We investigate the far-field scenario. The antenna elements are arranged as shown in Fig. 1, numbered from 1 to  $N$ . Let  $d = \lambda/2$ .

Given that the beampattern is a periodic function of  $\theta$ , we set  $\theta$  in a cycle interval of  $[0^\circ, 180^\circ]$ . Let  $\theta$ 's discrete value  $\theta_1, \theta_2, \dots, \theta_k, \dots, \theta_K$  be  $0^\circ, 1^\circ, \dots, 179^\circ, 180^\circ$ , in sequence. These settings are consistent with real practice and facilitate digital processing.

In the first example, let  $N=21$ , and the expected beampattern is created by uniform element excitation. The targeted beampattern can be obtained by:

$$s = \sum_{i=0}^{N-1} I e^{j2\pi i d (\cos \theta - \cos \theta_0) / \lambda}, \quad (24)$$

where  $\theta$  is the signal transmitting angle as shown in Fig. 1,  $\theta_0 = \pi/2$  is the scan angle, and  $I$  is the amplitude of the antenna element current excitation.

Let  $\mathbf{F} = \mathbf{P}$ ; the simulation outcomes are shown in Fig. 2. In the legend column of Fig. 2, the target denotes the expected beampattern created by equation (24); LS refers to the traditional least square solution of equation (6); eigen marks the synthesized beampattern that is the eigenvector to the eigenvalue of 1 obtained from eigenvalue decomposition of the matrix  $\mathbf{G}(\mathbf{G}^H \mathbf{G})^{-1} \mathbf{G}^H$ ; the beampattern of eigen is substituted into equation (23) to obtain the array element excitation and  $l=0, l=1, l=2, l=3, l=4$  indicate the beampatterns created by the element excitation of equation (23), while  $l$  has different values.

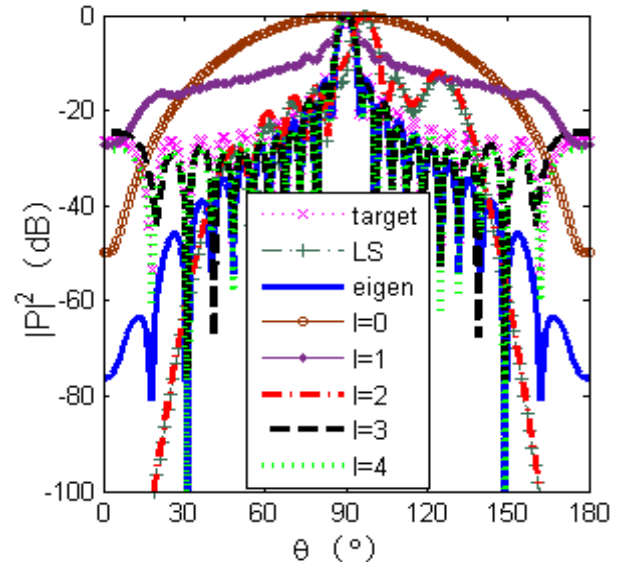


Fig. 2. The outcomes of the first simulation ( $N=21$ ).

In Fig. 2, the main-lobe of the targeted beampattern is in the range  $[84^\circ, 96^\circ]$ , with the highest level at  $\theta=90^\circ$ . Its first side-lobe peak level is  $-13.6$  dB. The main-lobe of the least square method is in the range  $[84^\circ, 106^\circ]$ , with the highest level at  $\theta=97^\circ$ . Its side-lobe peak level is  $-12.5$  dB at  $\theta=126^\circ$ . The beampattern of the eigenvalue decomposition method and the targeted beampattern overlap in range from the left second side-

lobe to the right second side-lobe. In the other range, while  $\theta$  is moving farther away from  $\theta=90^\circ$ , the gain of the eigenvalue decomposition beampattern gradually decreases more than that of the targeted beampattern. The beampattern created by equation (23), while  $l=0$ , has no apparent main-lobe or side-lobe. The beampattern, created by equation (23) while  $l=1$ , has an apparent main-lobe but no side-lobe. Its main-lobe is in the range of  $[85^\circ, 95^\circ]$ , with the highest level at  $\theta=90^\circ$ . Its first side-lobe peak level is -5.5 dB. While  $l=2$ , the beampattern created by equation (23) nearly overlaps with the beampattern of the least square method. The beampatterns created by equation (23), while  $l=3$  and  $l=4$ , nearly overlap with the targeted beampattern.

It can be seen from Fig. 2 that the synthesized beampattern from eigenvalue decomposition, and the outcomes, while  $l=3$ ,  $l=4$ , all have better agreement with the targeted beampattern than the outcome produced by the traditional least square method.

In the second example, let  $N=15$ , where all other conditions are the same as those in the first example. The expected beampattern is created by equation (24), with uniform element excitation. The simulation outcomes are shown in Fig. 3. In the legend column of Fig. 3, the target denotes the expected beampattern created by equation (24); LS refers to the traditional least square solution of equation (6); eigen marks the synthesized beampattern that is the eigenvector to the eigenvalue of 1 obtained from eigenvalue decomposition of the matrix  $\mathbf{G}(\mathbf{G}^H\mathbf{G})^{-1}\mathbf{G}^H$ ; the beampattern of eigen is substituted into equation (23) to obtain the array element excitation and  $l=0$ ,  $l=1$ ,  $l=2$ ,  $l=3$ ,  $l=4$  indicate the beampatterns created by the element excitation of equation (23), while  $l$  has different values.

In Fig. 3, the main-lobe of the targeted beampattern is in the range  $[82^\circ, 98^\circ]$ , with the highest level at  $\theta=90^\circ$ . Its first side-lobe peak level is -13.2 dB. The main-lobe of the least square method is in the range  $[90^\circ, 106^\circ]$ , with the highest level at  $\theta=97^\circ$ . Its side-lobe peak level is -1.5 dB at  $\theta=82^\circ$ . The beampattern of the eigenvalue decomposition method and the targeted beampattern overlap in the main-lobe range. In the other range, while  $\theta$  is moving farther away from  $\theta=90^\circ$ , the gain of the eigenvalue decomposition beampattern gradually decreases more than that of the targeted beampattern. The beampattern created by equation (23), while  $l=0$ , has no apparent main-lobe or side-lobe. The beampattern created by equation (23), while  $l=1$ , has an apparent main-lobe but no side-lobe. Its main-lobe is in the range  $[82^\circ, 98^\circ]$ , with the highest level at  $\theta=90^\circ$ . Its first side-lobe peak level is -5.3 dB. While  $l=2$ , the beampattern created by equation (23) nearly overlaps with the beampattern of the least square method. While  $l=3$  and  $l=4$ , the beampatterns created by equation (23) nearly overlap with the targeted

beampattern.

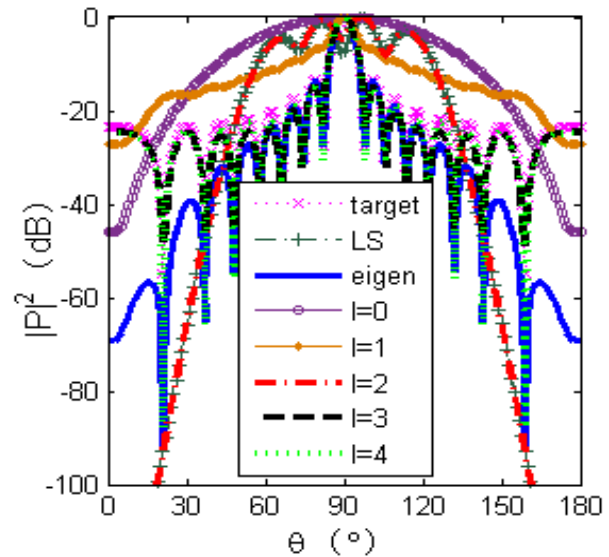


Fig. 3. The outcomes of the second simulation ( $N=15$ ).

It can be seen from Fig. 3 that, once again, the synthesized beampattern of eigenvalue decomposition, and the outcomes, while  $l=3$ ,  $l=4$ , all have better agreement with the targeted beampattern than the outcome produced by the traditional least square method.

In the third example, let  $N=23$ , and in the targeted beampattern, there exists a null beam, where  $\theta$  is in the scope from  $116^\circ$  to  $123^\circ$ , with a lowest attenuation of -81 dB at  $\theta=116^\circ$ . Except for these values, other conditions are the same as those in the first example. The expected beampattern is still created by equation (24), with uniform element excitation. The simulation outcomes are shown in Fig. 4. In the legend column of Fig. 4, the target denotes the expected beampattern created by equation (24); LS refers to the traditional least square solution of equation (6); eigen marks the synthesized beampattern that is the eigenvector to the eigenvalue of 1 obtained from eigenvalue decomposition of the matrix  $\mathbf{G}(\mathbf{G}^H\mathbf{G})^{-1}\mathbf{G}^H$ ; the beampattern of eigen is substituted into equation (23) to obtain the array element excitation and  $l=0$ ,  $l=1$ ,  $l=2$ ,  $l=3$ ,  $l=4$  indicate the beampatterns created by the element excitation of equation (23), while  $l$  has different values.

In Fig. 4, the main-lobe of the targeted beampattern is in the range  $[85^\circ, 95^\circ]$ , with the highest level at  $\theta=90^\circ$ . Its first side-lobe peak level is -13.5 dB. The main-lobe of the least square method is in the range  $[81^\circ, 95^\circ]$ , with the highest level at  $\theta=88^\circ$ . Its side-lobe peak level is -6.1 dB at  $\theta=113^\circ$ . The beampattern of the eigenvalue decomposition method and the targeted beampattern overlap in range from the left first side-

lobe to the right first side-lobe and null beam scope. In the other range, while  $\theta$  is moving farther away from  $\theta=90^\circ$ , the gain of the eigenvalue decomposition beampattern gradually decreases more than that of the targeted beampattern. The beampattern, created by equation (23), while  $l=0$ , has no apparent main-lobe or side-lobe. The beampattern, created by equation (23), while  $l=1$ , has an apparent main-lobe but no side-lobe. Its main-lobe is in the range  $[85^\circ, 95^\circ]$ , with the highest level at  $\theta=90^\circ$ . Its first side-lobe peak level is  $-6.7$  dB. While  $l=2$ , the beampattern created by equation (23) nearly overlaps with the beampattern of the least square method. While  $l=3$  and  $l=4$ , the beampatterns created by equation (23) nearly overlap with the targeted beampattern in the range where the null beam is not located. Only the targeted beampattern, the beampattern of the eigenvalue decomposition approach, and the beampattern created by equation (23), while  $l=4$ , have null beams in the same range; other beampatterns all have no null beam. The beampattern created by equation (23), while  $l=4$ , has a null beam with the lowest level,  $-79$  dB at  $\theta=116^\circ$ .

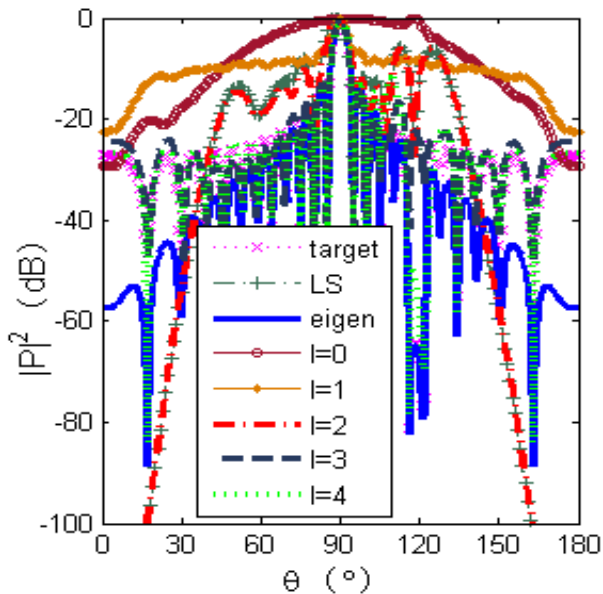


Fig. 4. The outcomes of the third simulation ( $N=23$ ).

It can be seen from Fig. 4 that, once again, both the synthesized beampattern from eigenvalue decomposition and the outcome, while  $l=4$ , have better agreement with the targeted beampattern than the outcome produced by the traditional least square method. In particular, at the null beam zone, both the beampattern synthesized from eigenvalue decomposition and the outcome, while  $l=4$ , have much better agreement with the targeted beampattern, and the outcome produced by the traditional least square method has no apparent null beam.

From these examples, we can learn that the new method has better performance than the traditional least square method, and while  $l$  increases from 1 to 4, the beampattern created by the element excitation of equation (23) gradually matches the targeted pattern better and better. We simulate the new approach using the MATLAB software platform on an HP notebook PC with a core i5-5200U CPU and a 4G memory. All simulations in this paper take approximately less than one second to obtain the final outcomes.

## VI. CONCLUSION

The synthesized beampattern can be obtained by eigenvalue decomposition of the projection matrix of the array manifold matrix, while the least square error reaches the minimum. For an antenna array whose manifold matrix has been determined, the projection matrix can be derived easily from the array manifold matrix. Then, eigenvalue decomposition of the projection matrix is conducted to obtain the synthesized beampattern, and the antenna element excitations can be solved by an ameliorated least square method. The results of the simulations compared with the traditional least square method show that the matching degree between the targeted beampattern and the synthesized beampattern of the new method is higher and that the new method is more efficient.

## ACKNOWLEDGMENT

This work has been supported in part by the Chinese Government under the grant No. 61501340 of the National Natural Science Foundation, and Education Department of Shaanxi Province under the grant No. 17JK0397 of the Special Research Plan of Science and Technology Foundation.

## REFERENCES

- [1] T. K. Sarkar, J. Koh, R. Adve, et al., "A pragmatic approach to adaptive antennas," *IEEE Acoust., Speech, and Signal Processing Mag.*, vol. 42, no. 2, pp. 39-55, 2000.
- [2] P. Lopez, J. A. Rodriguez, F. Ares, and E. Moreno, "Subarray weighting for difference patterns of monopulse antennas: Joint optimization of sub-array configurations and weights," *IEEE Trans. Antennas Propag.*, vol. 49, no. 11, pp. 1606-1608, 2001.
- [3] S. Caorsi, A. Massa, M. Pastorino, and A. Randazzo, "Optimization of the difference patterns for monopulse antennas by a hybrid real/integer coded differential evolution method," *IEEE Trans. Antennas Propag.*, vol. 53, no. 1, pp. 372-376, 2005.
- [4] M. D'Urso, T. Isernia, and E. F. Meliaddò, "An effective hybrid approach for the optimal synthesis of monopulse antennas," *IEEE Trans.*

- Antennas Propag.*, vol. 55, no. 4, pp. 1059-1066, 2007.
- [5] L. Manica, P. Rocca, A. Martini, and A. Massa, "An innovative approach based on a tree-searching algorithm for the optimal matching of independently optimum sum and difference excitations," *IEEE Trans. Antennas Propag.*, vol. 56, no. 1, pp. 58-66, 2008.
- [6] Y. Chen, S. Yang, and Z. Nie, "The application of a modified differential evolution strategy to some array pattern synthesis problems," *IEEE Trans. Antennas Propag.*, vol. 56, no. 7, pp. 1919-1927, 2008.
- [7] L. Manica, P. Rocca, M. Benedetti, and A. Massa, "A fast graph-searching algorithm enabling the efficient synthesis of sub-arrayed planar monopulse antennas," *IEEE Trans. Antennas Propag.*, vol. 57, no. 3, pp. 652-663, 2009.
- [8] A. Morabito and P. Rocca, "Optimal synthesis of sum and difference patterns with arbitrary sidelobes subject to common excitations constraints," *IEEE Antennas Wireless Propag. Lett.*, vol. 9, pp. 623-626, 2010.
- [9] H. He, P. Stoica, and J. Li, "Wideband MIMO systems: Signal design for transmit beampattern synthesis," *IEEE Trans. Signal Processing*, vol. 59, no.2, pp. 618-628, 2011.
- [10] G. Oliveri and A. Massa, "Bayesian compressive sampling for pattern synthesis with maximally sparse non-uniform linear arrays," *IEEE Trans. Antennas Propag.*, vol. 59, no. 2, pp. 467-481, 2011.
- [11] X. Li, W. T. Li, and X. W. Shi, "Modified differential evolution strategy for antenna array pattern synthesis," *Progr. Electromagn. Res.*, vol. 137, no. 2, pp. 371-388, 2013.
- [12] H. Chen, Q. Wang, and R. Fan, "Beampattern synthesis using reweighted  $l_1$ -norm minimization and array orientation diversity," *Radioengineering*, vol. 22, no. 2, pp. 602-609, 2013.
- [13] R. L. Haupt, "Phased array beam steering through serial control of the phase shifters," *Appl. Comput. Electrom. Society Journal*, vol. 32, no. 12, pp. 1140-1143, 2017.
- [14] L. I. Vaskelainen, "Constrained least-squares optimization in conformal array antenna synthesis," *IEEE Trans. Antennas Propag.*, vol. 55, no. 3, pp. 859-867, 2007.
- [15] J. Chen, Y. Z. Yin, and Y. Jiao, "A steerable least square approach for pattern synthesis," *Progr. Electromagn. Res. M*, vol. 59, pp. 181-191, 2017.
- [16] J. Capon, "High resolution frequency-wave number spectrum analysis," *Proceedings of the IEEE*, vol. 57, pp. 1408-1418, 1969.
- [17] J. Nourinia, C. Ghobadi, B. Mohammadi, and F. Alizadeh, "Study of phase and patterns

characteristics of a sub-wavelength broadband reflectarray unit element based on triple concentric circular-rings," *Appl. Comput. Electrom. Society Journal*, vol. 33, no. 6, pp. 714-718, June 2018.



**Jie Chen** is now an Associate Professor of School of Electronic Engineering, Xi'an Aeronautical University, No.259 Xi'an West Second Ring Road, Xi'an, 710077, China. He received his bachelor and master degree in Electronic Science and Technology major from School of Electronic and Information, Xi'an Jiaotong University in 1997 and 2004, respectively. In 2013, he achieved his doctor degree in Electromagnetic Theory and Microwave Technique major from School of Electronic Engineering, Xidian University. His research interests are in the areas of smart antenna, antenna array, microwave circuit design, wireless communication and RFID technique.



**Yingzeng Yin** is now a Professor of Xidian University. He works in National Key Laboratory of Antenna and Microwave Technology, School of Electronic Engineering, Xidian University, Xi'an, 710071, China. His research activities are in the fields of microwave circuit design, antenna design, smart antenna design and RFID technique.